IL NUOVO CIMENTO **47 C** (2024) 76
DOI 10.1393/ncc/i2024-24076-1

Colloquia: IFAE 2023

Latest VBS and VBF results with the ATLAS and CMS experiments(*)

Benedetta Camaiani on behalf of the ATLAS and CMS Collaborations
Department of Physics and Astronomy - Via G. Sansone 1, 50019 Sesto Fiorentino (FI), Italy

received 13 February 2024

Summary. — Vector Boson Scattering and Fusion processes are crucial to probe the electroweak sector of the Standard Model, as they are sensitive to self-couplings of vector bosons. This review summarizes the latest measurements of production cross sections of vector bosons in association with two jets, performed using data collected by the ATLAS and CMS experiments at $\sqrt{s} = 13$ TeV during the LHC Run 2 data taking period.

1. – Introduction

The discovery of the Higgs boson by the ATLAS [1] and CMS [2] Collaborations has set off several precision measurements of the electroweak (EW) sector of the Standard Model (SM). In particular, the high energy and luminosity reached by the Large Hadron Collider (LHC) during the Run 2 data taking period, have allowed the rare vector boson scattering (VBS) and fusion (VBF) processes to be studied in detail. The multi-boson VBS production is particularly interesting to study because its amplitude strongly depends on the coupling between vector bosons and the Higgs boson, therefore, it represents a key process to understand the properties of the EW symmetry breaking mechanism. Moreover, if this coupling deviates from the SM prediction, VBS amplitudes would diverge in the high energy limit, violating the theory unitarity.

This note provides a summary of some of the most recent VBF and VBS results, performed by the ATLAS and CMS Collaborations using data collected during the LHC Run 2 at $\sqrt{s} = 13$ TeV and corresponding to an integrated luminosity of $\mathcal{L} \simeq 140$ fb^{-1}.

2. – Measurement of the electroweak $Z\gamma$ production

Among the VBS processes, the $Z\gamma$ production has a crucial role being one of the few processes sensitive to the neutral quartic gauge couplings. The ATLAS collaboration has recently performed the measurement of the electroweak $Z\gamma$ production, in association with two hadronic jets [3]. The measurement is performed by selecting events in which the

(*) IFAE 2023 - "Energy Frontier" session

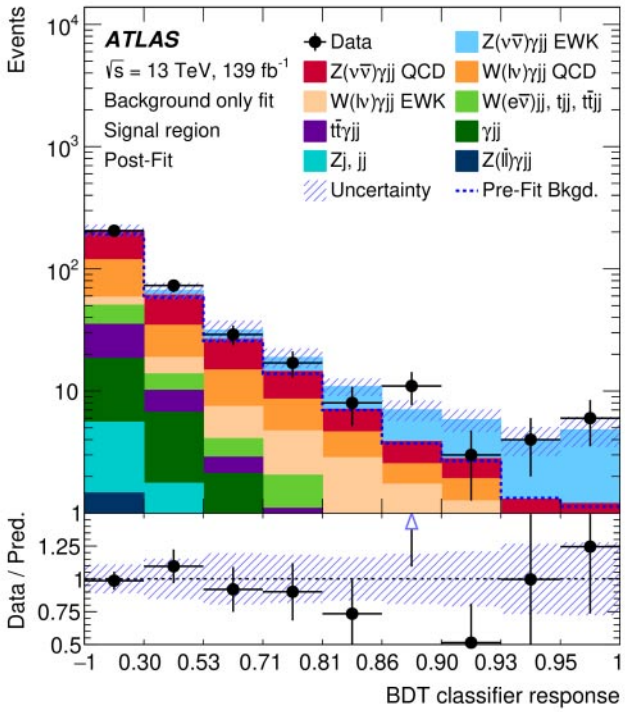

Fig. 1. – Post-fit distribution of the BDT classifier evaluated in the signal region of the electroweak $Z(\nu\bar{\nu})\gamma jj$ production [3].

Z boson decays into two neutrinos ($\nu\bar{\nu}$) and in a high-energy regime, defined by requiring the photon transverse momentum to be above 150 GeV, in order to have more sensitivity to possible anomalous quartic gauge couplings (aQGCs). The main backgrounds for the selected final state are the $Z(\nu\bar{\nu})\gamma jj$ QCD-induced production and the $W(\ell\nu)\gamma jj$ QCD- and EW-induced production. Both contributions are measured in dedicated control regions. The signal selection is carried out using a boosted decision tree (BDT), that takes as input the kinematics variables related to the dijet system and the photon of the final state. Finally, the signal is extracted through a maximum likelihood template fit, using the BDT score distribution as fit variable in the signal region and the invariant mass of the dijet system in the control regions. Figure 1 reports the post-fit distribution of the BDT classifier response. The cross section is measured within a fiducial phase space, defined to closely follow the reconstructed-level selection. The observed cross section is $\sigma_{Z\gamma EWK} = 0.77^{+0.34}_{-0.30}$ fb, which is in agreement with the SM predictions at next-to-leading order in perturbative QCD. This measurement has allowed the evidence of the $Z\gamma$ process with an observed signal significance of 3.2σ, that grows up to 6.3σ when combined with the previous ATLAS result performed in the low-energy regime [4].

Since no deviations from the SM expectations have been found, the data have been used to set limits on aQGCs. In particular, the effective field theory (EFT) dimension-8 operators have been considered, and the constraints are either competitive with or more stringent than those previously published by the ATLAS and CMS collaborations.

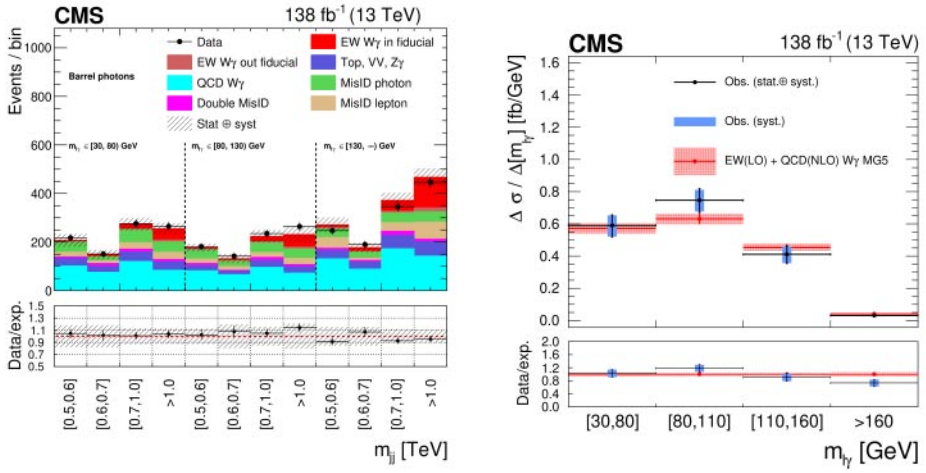

Fig. 2. – Distributions of the 2D fit variable ($m_{\ell\gamma} - m_{jj}$) in the barrel region (left) and differential cross section distribution for the EW+QCD $W\gamma$ production as a function of the lepton-photon pait invariant mass $m_{\ell\gamma}$ (right) [5].

3. – Measurement of the electroweak $W\gamma$ production

In the context of VBS measurements, one of the latest CMS results is about the $W\gamma$ production in association with two hadronic jets [5]. The measurement targets the EW $W\gamma$ process, selecting events in which the W boson decays into a charged lepton and a neutrino. A measurement of the EW- and QCD-induced production is also reported. The main background of the EW production is due to the $W\gamma$ process via QCD, that is measured using a dedicated control region. Other important background contributions arise from W+jets events and events involving top quark where the jet constituents are misidentified as a photon. The signal is extracted through a binned likelihood fit to the data, using a 2D fit variable composed of the invariant mass of the lepton-photon pair ($m_{\ell\gamma}$) and the invariant mass of the dijet system (m_{jj}). The choice of the fit variable is dictated by the fact that both $m_{\ell\gamma}$ and m_{jj} have high discriminating power between the EW- and QCD-induced $W\gamma$ production. Figure 2 (left) shows the distributions of the 2D fit variable in the barrel region.

The measurement provides the first observation of the EW $W\gamma$ signal at 13 TeV, with an observed significance of 6.0σ. Moreover, both the EW and total $W\gamma$ production are measured in a restricted fiducial region and are consistent with the SM predictions.

For the first time, differential measurements of the EW and total $W\gamma$ component are also performed as a function of several kinematics observables. The differential distribution of the total production as a function of the lepton-phton pair invariant mass is shown as an example in fig. 2 (right).

Finally, the EW signal component is used to set limits on aQGC in terms of dimension-8 EFT operators. In particular, the limits set to the parameters $f_{\mathrm{M},2-5}/\Lambda^4$ and $f_{\mathrm{T},6-7}/\Lambda^4$ are the most stringent to date.

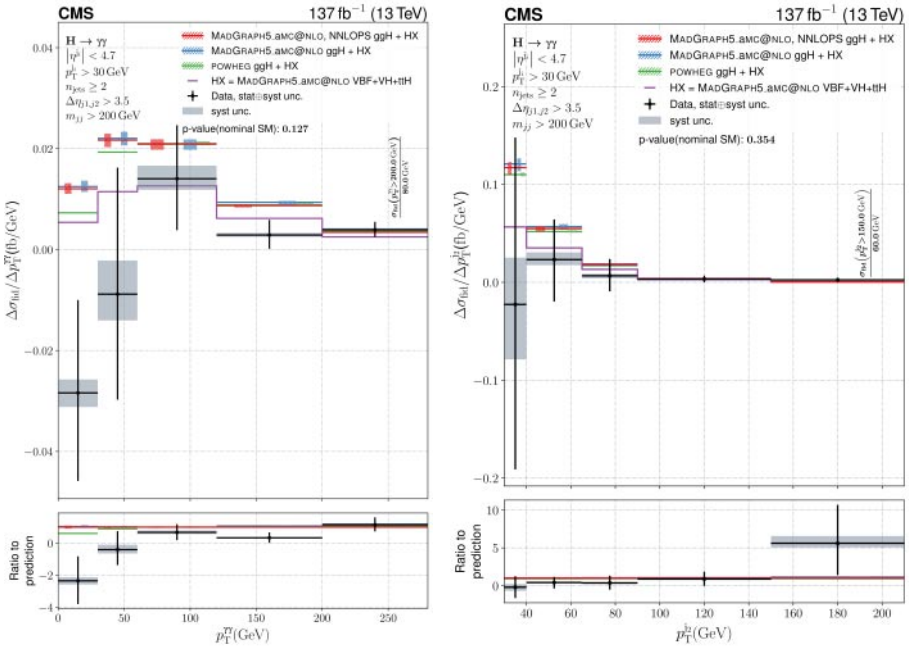

Fig. 3. – Fiducial differential cross sections as a function of $p_T^{\gamma\gamma}$ (left) and $p_T^{\gamma\gamma}$ (right) measured in the VBF-enriched phase space [6].

4. – Inclusive and differential cross section measurements in $H \to \gamma\gamma$

The high precision in the reconstruction of the diphoton invariant mass makes the $H \to \gamma\gamma$ decay channel very suitable for measuring Higgs boson differential production cross sections. The most recent result performed by the CMS collaboration in this decay channel [6] consists of the measurement of twenty differential cross sections, some of them performed also in a VBF-enriched phase space. To reduce their model dependence, inclusive and differential production cross sections are measured in a fiducial phase space, defined by means of cuts on the single photons and to the diphoton system. In addition to this baseline selection, a 2-jets phase space is defined using additional cuts on the dijet system, in order to design a region enriched in VBF Higgs boson production events. Finally, the signal is extracted using the diphoton invariant mass as fit variable.

The inclusive cross section measured within the fiducial volume is consistent with the SM prediction within one standard deviation. Two differential distributions among the extensive set of results are reported in fig. 3, where the cross section is measured in the VBF-enriched phase space as a function of transverse momentum of the dijet system $p_T^{\gamma\gamma}$ (left) and of the subleading jet $p_T^{j_2}$ (right). The per-bin uncertainties can reach 150%. Overall, an under fluctuation is observed for the events entering the VBF region.

5. – CP property of the Higgs boson to electroweak boson coupling in $H \to \gamma\gamma$

The ATLAS Collaboration has recently published a test of CP invariance in Higgs boson production through the VBF mechanism, targeting events in which the Higgs boson decays into two photons [7]. Following an EFT approach, a CP-odd component in the

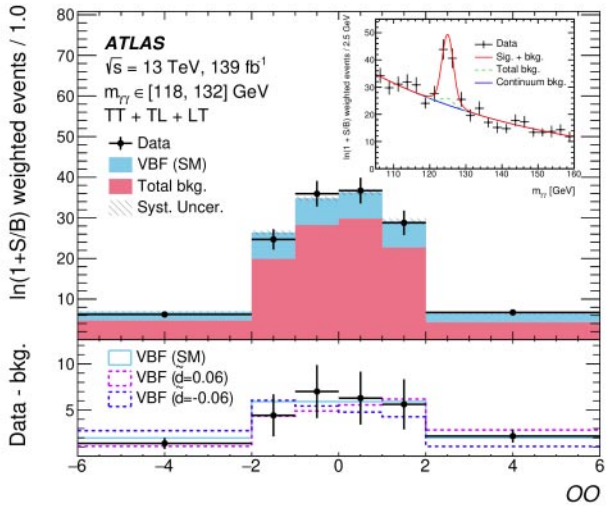

Fig. 4. – Distribution of the optimal observable OO, including events coming from the three signal regions [7].

Higgs boson coupling to vector bosons (vertex $HVV, V = W, Z$) can be parametrized by adding dimension-6 operators to the Lagrangian of the SM. The CP violation contribution can be distinguished using a CP-odd observable. In this study, the optimal observable (OO) defined as follow is adopted:

$$OO = 2 \cdot \mathrm{Re}(\mathcal{M}^{*}_{\mathrm{SM}} \cdot \mathcal{M}_{\mathrm{CP-odd}})/|\mathcal{M}_{\mathrm{SM}}|^{2} \tag{1}$$

where $\mathcal{M}_{\mathrm{SM}}$ and $\mathcal{M}_{\mathrm{CP-odd}}$ represent the SM and CP-odd contribution, respectively. According to the SM, the OO distribution is symmetric with a mean value of zero. Therefore, any asymmetrical behaviour would indicate contributions from the CP violation term. Results of this analysis are interpretated in the EFT HISZ and Warsaw bases.

To maximize the sensitivity to the VBF signal, two BDT classifiers have been trained using observables related to the dijet and diphoton systems as input features. The first one is used to discriminate the signal from the gluon-gluon Higgs boson production, whereas the second one to recognize the continuum background contribution. Three different signal regions have been defined using the output of the BDTs and finally, the signal has been extracted through a combined unbinned maximum-likelihood fit to the diphoton invariant mass spectra split into the OO bins. Figure 4 shows the distribution of the OO observable, including contributions from the three signal regions. The results are compatible with the SM prediction and no sign of CP violation is observed in the OO distribution. The constraints set in parameters describing the CP-odd component of the HVV vertex are the most stringent to date. In particular, 95% confidence level intervals are set on the $\tilde{d}$ operator of the HISZ basis for the first time and the constraints on the opertator $c_{H\tilde{W}}$ of the Warsaw basis is more restrictive by a factor of two than ATLAS and CMS previous results in the four leptons channel.

6. – Conclusions

The amount of data collected by the ATLAS and CMS experiments during the LHC Run 2 has allowed to measure vector boson scattering and fusion processes with a very high level of precision. This note presents a brief outlook of the most recent results from the ATLAS and CMS Collaborations. Results are shown in the form of inclusive and differential cross sections, and no significant deviations from the SM predictions have been found. Constraints on the anomalous quartic gauge couplings in terms of dimension-8 effective field theory operators are also set and some of them are the most stringent results to date.

REFERENCES

[1] ATLAS Collaboration, *JINST*, **3** (2008) S08003.
[2] CMS Collaboration, *JINST*, **3** (2008) S08004.
[3] ATLAS Collaboration, *J. High Energy Phys.*, **2023** (2023) 82.
[4] ATLAS Collaboration, *Eur. Phys. J. C*, **82** (2023) 105.
[5] CMS Collaboration, *Phys. Rev. D*, **108** (2023) 032017.
[6] CMS Collaboration, *J. High Energy Phys.*, **2023** (2023) 91.
[7] ATLAS Collaboration, *Phys. Rev. Lett.*, **131** (2023) 061802.